Rock Mech Rock Eng (2016) 49:4919–4928
DOI 10.1007/s00603-016-1034-9

TECHNICAL NOTE

Shear Behaviour and Acoustic Emission Characteristics of Different Joints Under Various Stress Levels

Fanzhen Meng[1,2] · Hui Zhou[2] · Shaojun Li[2] · Chuanqing Zhang[2] · Zaiquan Wang[1] · Liang Kong[1] · Liming Zhang[1]

Received: 28 July 2015 / Accepted: 19 June 2016 / Published online: 24 June 2016

Keywords Joint · Shear strength · High normal stress · Shear stress drop · Acoustic emission (AE)

1 Introduction

Rock masses are typically characterised by faults, joints, bedding planes and other planes of weakness, and the mechanical behaviours (such as shear strength, stiffness, deformation and permeability) of jointed rock masses strongly depend on the mechanical and geometric properties of discontinuities. Shear failure along weak joints is one of the main failure modes in rock slopes and underground excavations; thus, understanding and predicting the shearing behaviours of jointed rockmasses are important for the design and stability analysis of rock structures. Patton (1966) proposed a bilinear strength envelope that describes the shear strength of saw-tooth joints well. Ladanyi and Archambault (1969) developed a new model by identifying the areas on the joint surface where sliding and breaking of asperities are most likely to occur. Based on a series of shear tests conducted on natural rough joints, Barton and Choubey (1977) introduced an empirical model that includes three index parameters: the joint roughness coefficient, the joint wall compressive strength and the residual friction angle. Zhao (1997) modified Barton and Choubey's criterion by introducing the joint-matching coefficient. With the development of optics and data processing technology in recent years, the surface morphology of joints can be quantitatively investigated, and some new empirical criteria have been proposed by considering three-dimensional quantified surface roughness parameters (Grasselli 2006; Xia et al. 2014). Model materials (plaster, cement mortar) have mainly been used in previous studies to simulate rock joint, and the normal stresses applied were typically low as the burial depths of the engineering rock are generally shallow. Presently, the excavation depths of many tunnels extend beyond depths of 1000 or 2000 m, with high stress levels acting on the discontinuities. Therefore, it is important to understand the shear behaviour of joints under high normal stress.

Real-time monitoring of joint shearing is an important issue that must be addressed to understand the evolution of the shearing process and its underlying failure mechanisms and predict imminent shear failure. The acoustic emission (AE) technique has been widely applied to monitor and predict the failure processes of rock materials, and few researchers have addressed the application of AEs for monitoring the shear behaviour of joints (Hong and Seokwon 2004; Moradian et al. 2010, 2012; Zhou et al. 2014; Meng et al. 2016). However, studies of the AE characteristics of joints during shear failure, especially for rough joints under high normal stress, remain scarce.

In this study, shear tests under constant normal loading (CNL) on tensile joints in three different types of rock were carried out, the shear behaviours of the joints were studied, and the changes in the AEs that occurred during shear failure under different normal stresses were investigated. The strength characteristics were analysed, and the AEs were recorded and compared among the different types of joints and the different normal stresses.

✉ Hui Zhou
hzhou@whrsm.ac.cn

[1] College of Science, Qingdao University of Technology, Qingdao 266033, Shandong, China

[2] State Key Laboratory of Geomechanics and Geotechnical Engineering, Institute of Rock and Soil Mechanics, Chinese Academy of Sciences, Wuhan 430071, Hubei, China

2 Experimental Programme

Granite, marble and rock-like materials consisting of cement mortar, which can represent very hard rock, intermediate hard rock and soft rock, respectively, were used in this study. The basic mechanical parameters of the three different rock types are given in Table 1. Cubic samples of granite with 10-cm-long sides were cut from a long piece of granite and then ground to produce parallel opposite faces according to the suggested methods of the International Society for Rock Mechanics (ISRM). Marble was sampled from the Jinping II hydropower station and processed using the same methods and standards that were used for granite. The model material is a mixture of cement, fine quartz sand and water at a weight ratio of 1:1:0.5. The large block was cured at room temperature for one month and then cut with a saw into cubic $10 \times 10 \times 10$ cm samples. The cubic specimens were split by applying a pair of knife-edge loads to the middle of the sample, and joints with rough surfaces and interlocking asperities were made.

Shear tests were performed at the Institute of Rock and Soil Mechanics, Chinese Academy of Sciences using an RMT150C testing machine. The maximum normal and shear load values were 1000 and 500 kN, respectively. During the tests, normal load was applied at a rate of 1 kN/s and then held constant, and a shear load was subsequently applied at a rate of 0.005 mm/s. AEs were monitored using a 16-channel PAC-DISP system, and four PICO sensors were attached to the three sides of the low part of the joint in a plane (approximately 0.5 cm from the joint surface). A layer of the couplant was painted on the interface between the rock and sensors. The resonant frequency and operating frequency range of the sensors were 500 and 200–750 kHz, respectively, and the sampling rate was 1 million samples per second. The amplification of the preamplifier and the threshold of the system were both 40 dB. To ensure that the shearing process was synchronised with the AE acquisition process, the AE system was simultaneously triggered when the shear stress was applied. Some of the prepared samples, the arrangement of the AE sensors, and the experimental system are shown in Fig. 1. The normal stresses that were applied to the three different joints during the shear tests are provided in Table 1.

3 Experimental Results

3.1 Shear Behaviours of the Three Different Types of Joints

The shear stress curves of the cement mortar, marble and granite joints under low and high normal stresses are, respectively, illustrated in Fig. 2 to show the differences of the shear stress curves from low to high normal stresses. In general, the shear stress of the cement mortar joints under different normal stresses varied with shear displacement in a stable state, as shown in Fig. 2a, b, and no noise was emitted during the shear process. At normal stresses lower than 5 MPa, distinct peak shear stresses can be identified in the stress curves, and the shear stress gradually and steadily decreases to the ultimate shear strength with shear displacement. At normal stresses higher than 7 MPa, the stress curves in the post-peak period are irregular and show some fluctuations due to local fractures and concentrated damage at the irregular joint surface.

Figure 2c, d illustrates the shear stress curves for the marble joints. The shapes of the stress curves are similar and are characterised by their smoothness and inconspicuous strain weakening. In addition, the failure process of all of the joints was quiet and slow, and the macroscopic shear behaviours of the marble joints under low and high normal stress conditions were similar.

The shear stress versus shear displacement curves of the granite joints are shown in Fig. 2e, f. At normal stresses lower than 3 MPa, the shear stress increased to a peak value and then slowly decreased to the ultimate shear strength. As the normal stress increased, the shear stress at the peak drastically decreased to a terminal point, which was accompanied by a loud sound, and then increased again with shear displacement to a relative peak value before subsequently decreasing to the ultimate shear strength. At normal stresses greater than 10 MPa, violent post-peak stress drop and periodic shear stress oscillations with instantaneous small shear stress drops occurred simultaneously, which were not observed in the cement mortar and marble joints. In addition, continuous noises were emitted from the shear boxes, and each small stress drop corresponded with a loud sound, which indicated that large amounts of energy were being released. Unstable sliding occurred because the loading system (with soft

Table 1 Basic mechanical parameters and normal stresses for three different kinds of joints that were applied in the shear tests

Type of joint	σ_c (MPa)	E (GPa)	μ	Normal stress/MPa
Cement mortar	46.39	7.28	0.077	0.5, 1, 2, 3, 5, 7, 10, 14, 20
Granite	191.24	20.74	0.132	1, 3, 5, 7, 10, 20, 30, 40, 45
Marble	95.27	17.56	0.074	1, 5, 7, 10, 15, 20, 30, 40

σ_c, E and μ are uniaxial compression strength, elastic modulus and poisson ratio, respectively

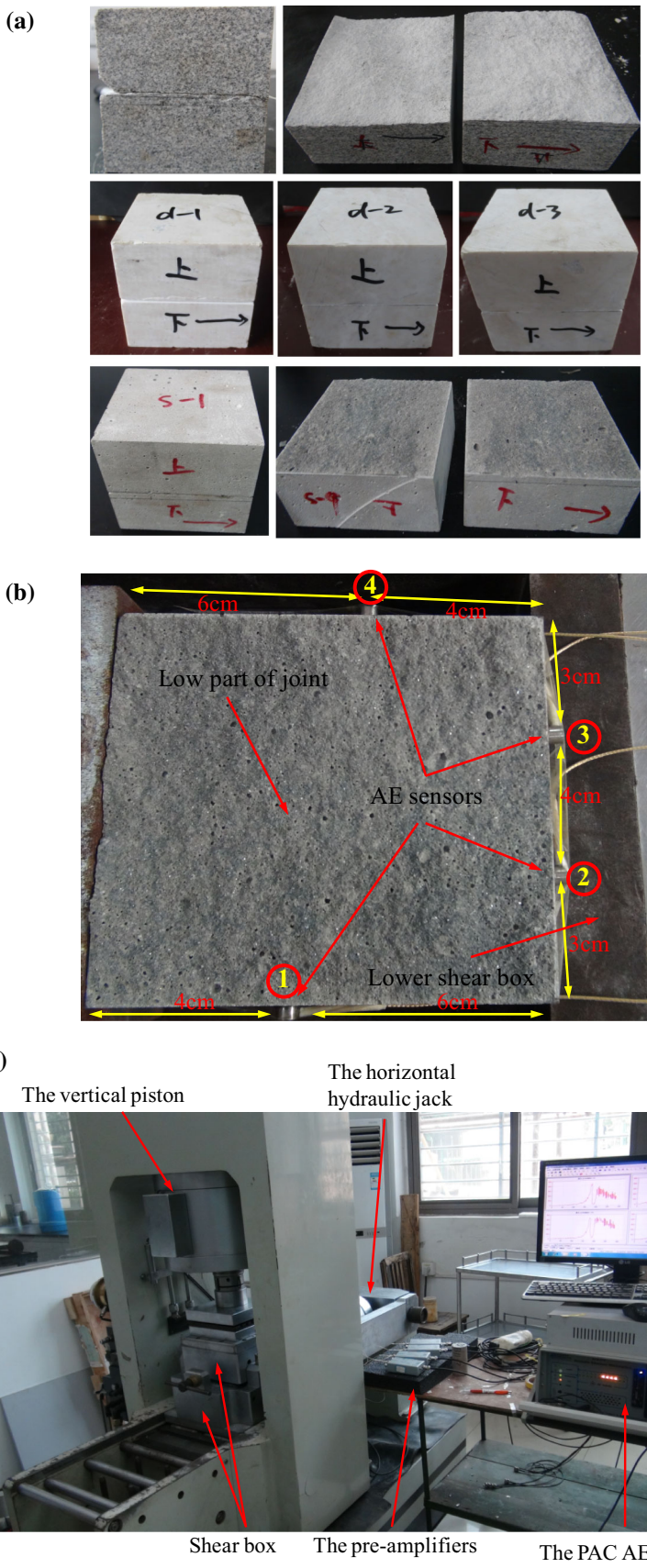

Fig. 1 Joint samples and the experimental system. **a** Some of the prepared joints (from *top to bottom*: granite joints, marble joints and cement mortar joints); **b** arrangement of the AE sensors (the Arabic numbers in the *circles* indicate the sensor numbers); **c** the RMT150C experimental system and the AE system during shear tests

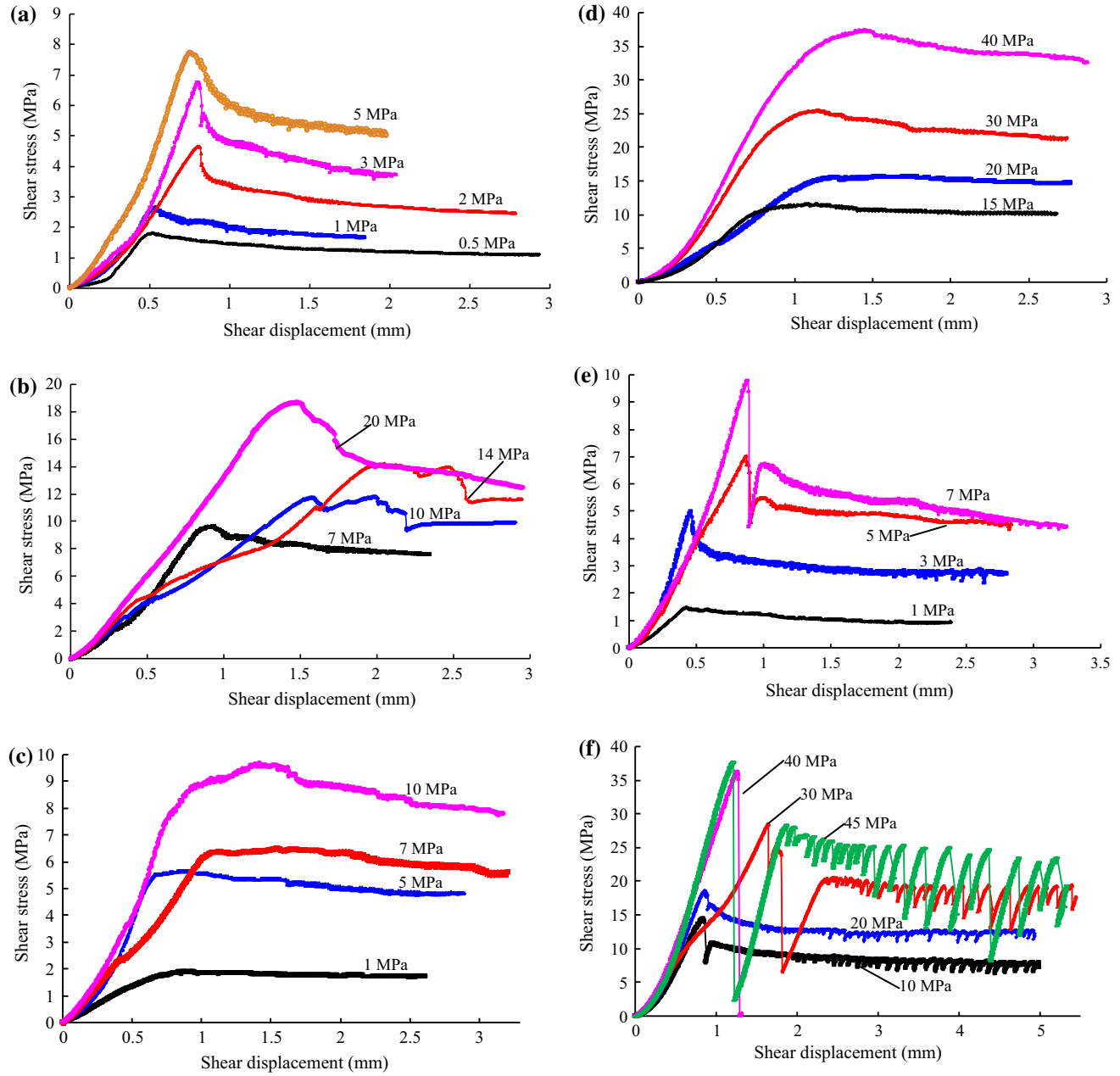

Fig. 2 Curves of shear stress versus shear displacement for cement mortar joints (**a**, **b**), marble joints (**c**, **d**) and granite joints (**e**, **f**) under different normal stresses

loading system stiffness) was not capable of responding rapidly enough to the rapid fracturing of the rock (Scholz 2002). According to the simulation study using the distinct element method by Bewick (2013), the fracturing events that occur during stress drops show increasing fracture rates with both grain boundary and intra-grain fracturing occurring simultaneously, and the cumulative fracture count curves show steps at each of the oscillations. This result indicates that as dilation was prevented under higher levels of normal stress, the asperities on the granite joint built substantial apparent cohesion, whereas the fractures led to sudden cohesion loss and ultimately resulted in stress drops.

3.2 Strength Characteristics of Three Different Types of Joints

The peak and ultimate shear strengths and corresponding normal stresses of the three different types of joints are shown in Fig. 3. The peak shear strengths of the cement mortar joints and granite joints are well described by the bi-linear model proposed by Patton (1966):

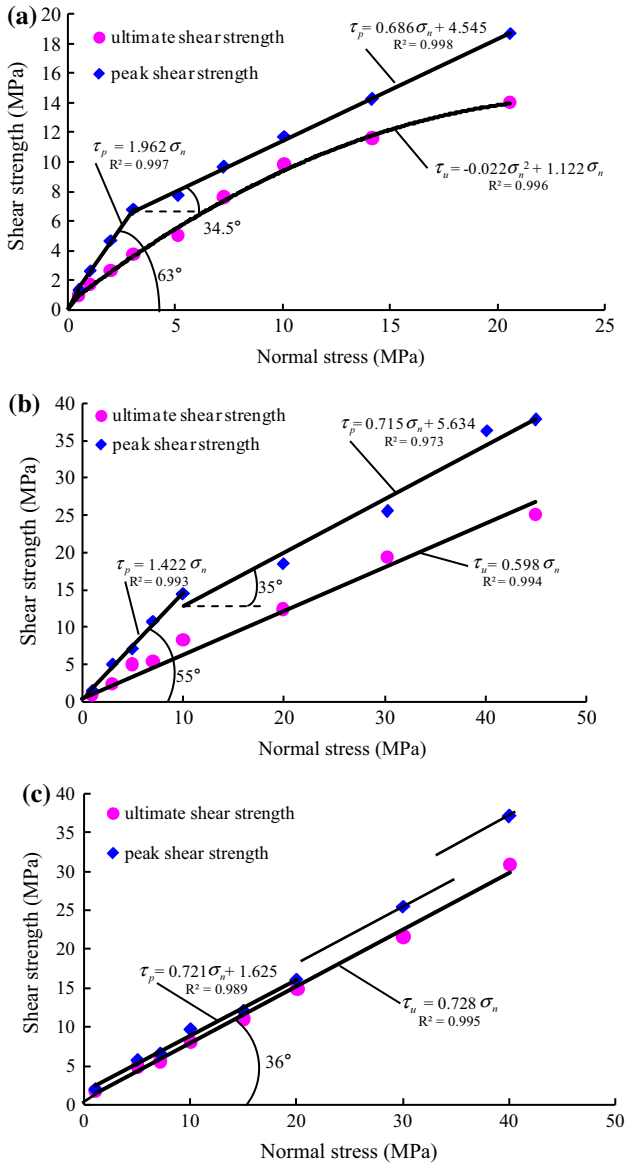

Fig. 3 Peak and ultimate strength envelopes for the **a** cement mortar joints, **b** granite joints and **c** marble joints

$$\tau_p = \sigma_n \tan(\phi + i) \quad \text{(when normal stress is low)} \tag{1}$$

$$\tau_p = \sigma_n \tan\phi + c \quad \text{(when normal stress is high)} \tag{2}$$

where τ_p, σ_n, ϕ, i and c are the peak shear strength, normal stress, friction angle, dilation angle and apparent cohesion, respectively (Patton 1966). The peak shear strength can be described as follows:

For cement mortar joints:

$$\tau_p = 1.962\sigma_n, \quad \sigma_n \le 3\,\text{MPa} \tag{3}$$

$$\tau_p = 0.686\sigma_n + 4.545, \quad 3\,\text{MPa} < \sigma_n \le 20\,\text{MPa} \tag{4}$$

For granite joints:

$$\tau_p = 1.422\sigma_n, \quad \sigma_n \le 10\,\text{MPa} \tag{5}$$

$$\tau_p = 0.715\sigma_n + 5.634, \quad 10\,\text{MPa} < \sigma_n \le 45\,\text{MPa} \tag{6}$$

Experimental data indicated that the ultimate shear strength of the cement mortar increased at a slower rate with increasing normal stress, which can be fit using the following quadric relationship:

$$\tau_u = -0.022\sigma_n^2 + 1.122\sigma_n, \quad 0\,\text{MPa} \le \sigma_n \le 20\,\text{MPa} \tag{7}$$

The curved nature of the strength envelope indicated that the mortar was collapsing under elevated normal stress because of its high porosity and loose structure, which resulted in higher initial friction (the slope of the strength envelope).

For the granite joint, the ultimate shear strength increased linearly with increasing normal stress due to the hard and brittle mineral constituents with high strength and can be expressed using the following linear formula:

$$\tau_u = 0.598\sigma_n, \quad 0\,\text{MPa} \le \sigma_n \le 45\,\text{MPa} \tag{8}$$

The ultimate strength of the marble joint increased linearly with normal stress in the range of the normal stress applied in this study and was fit using the following formula:

$$\tau_u = 0.728\sigma_n, \quad 0\,\text{MPa} \le \sigma_n \le 40\,\text{MPa} \tag{9}$$

Compared with the cement mortar and granite joints, the peak strength envelope of the marble joints showed unique characteristics. When the normal stress was less than 20 MPa, the peak strength increased linearly as follows:

$$\tau_p = 0.721\sigma_n + 1.625, \quad \sigma_n \le 20\,\text{MPa} \tag{10}$$

Equations (9) and (10) show that the slopes of the two fitted strength lines are almost identical, indicating that dilation was not obvious for the marble joints, and the apparent cohesion was 1.625 MPa. When the normal stresses were 30 and 40 MPa, the shear strengths were slightly higher than expected. If two lines are drawn that pass through the two strength points with the same slope as the ultimate strength envelope, the intercepts of the two lines with the vertical axis (namely, apparent cohesion) are 3.56 and 7.88 MPa, as shown in Fig. 3c. Because the roughnesses of these two joints are similar to those sheared under low normal stresses, the higher shear strengths did not result from the differences between the joint surfaces. Barton (1973) found that the shear strength of a joint would increase under high normal stress due to the over-closure effect, which can be used to explain the higher strength here because the two parts of the marble joint cannot be pried apart easily after shear failure. Unlike granite, marble is composed of minerals that can yield and soften under high stress levels; thus, these locked asperities on the two surfaces are absorbed tightly, and the joints were mechanically over-closed, which increased the adhesion force (apparent cohesion). Consequently, the apparent

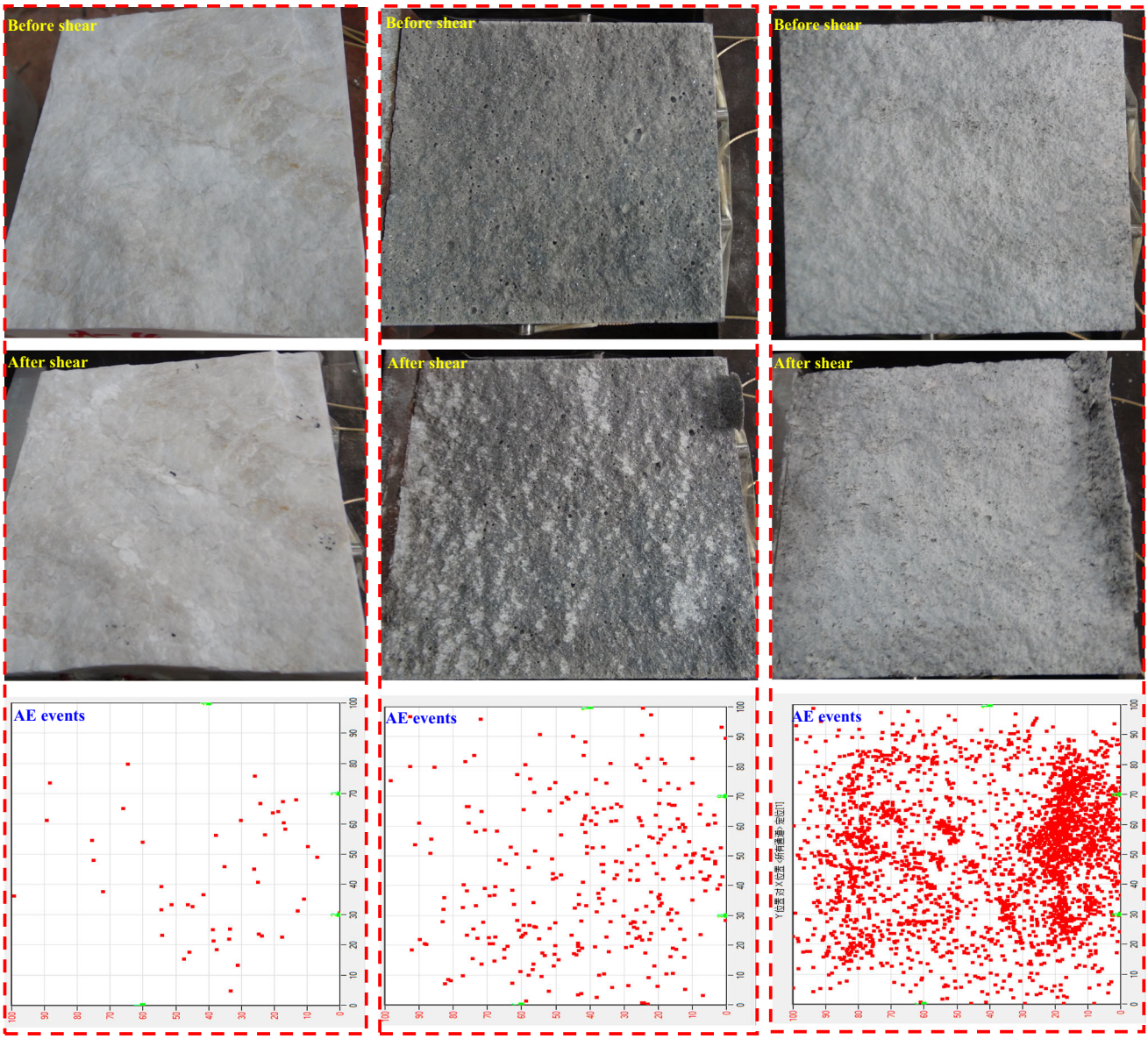

(a) Marble joint **(b)** Cement mortar joint **(c)** Granite joint

Fig. 4 Comparison of the joint surfaces before and after shear and the locations of AE events for the three different rock joints when normal stress was applied at 1 MPa (the *green points* indicate the positions of the sensors) (color figure online)

cohesion is greater at higher normal stress levels for marble joints.

The abrupt changes in the slopes of the two peak strength lines represent the transition of the shear failure mode (Patton 1966) from dilation with little or no asperity shearing under low normal stress to non-dilation when the tips of most of the asperities were sheared off under high normal stress. As shown in Fig. 3, the transition normal stress for cement joints was 3 MPa, which was lower than the transition normal stress of 10 MPa for granite joints. This difference reflects the lower shear-off resistance of the cement asperities. Because the vertical distance between a point on any maximum strength failure envelope and the ultimate envelope represents the internal strength contributed by the irregularities (i.e. the apparent cohesion loss), the cohesion loss was the greatest for granite joints, as shown in Fig. 3, which was consistent with the most violent brittle failure phenomena.

The dilation angle i is equal to the difference between the inclination angles of the two straight peak shear strength lines. The i values of the cement mortar and granite were 28.5° and 20°, respectively, and indicated that dilation was the most pronounced for the cement mortar

joints and the least pronounced for the marble joints when the normal stress was low. The dilation of the rock joint was closely related to the morphology of the joint surface under low normal stress. The damage distribution of the asperities during shearing can be investigated using the locations of the AE events. Figure 4 shows the joint surfaces before and after shearing and the locations of the AE events for the three different rock joints under a normal stress of 1 MPa. The marble joint had the fewest AE events, and the granite joint had the most AE events. The marble joint surfaces were smooth and slippery, and the granite and cement joint surfaces were rough and prickly before shearing, which indicated the presence of large numbers of small-scale sharp asperities due to tensile fracturing of the mineral grains on the surfaces of the granite and cement joints. Therefore, the lack of small-scale asperities on the marble joint surfaces caused the fewest AE events and the lowest dilation. On both surfaces of the granite and cement mortar joints, there are lots of tiny asperities in addition to the macroscopic fluctuations, and the mineral grains in the granite were more brittle and stiff than those in the cement mortar joint. Thus, the AEs were much more active for granite joints under the same normal stress.

3.3 Acoustic Emissions of Three Different Types of Joints Under Low and High Normal Stresses

It is necessary to monitor the shear behaviours of joint samples in the laboratory with morphological features that are similar to actual joints in order to apply AE for monitoring the shear behaviour of in situ discontinuities and to employ the AE technique for predicting the shear failure of rock joints. Below, the representative monitoring results of three different types of joints subjected to low and high normal stresses are presented and compared.

The AEs resulting from 1 and 10 MPa of normal stress, which represent smooth (normal stress lower than 7 MPa) and rough stress curves (normal stress higher than 10 MPa), respectively, are shown as examples of the AE characteristics of cement mortar joints in Fig. 5. The hit/energy rates of 1, 2, 3 and 4 in the graphs indicate the AE counts/energy recorded by the first, second, third, fourth sensors, respectively, in one second. The AE energy parameters (energy rate and cumulative energy) in the PAC software represent the relative energy or intensity of the AE hit, which is defined as the area enclosed by the signal envelope (unit of voltage is mv) and the axis of the abscissas (unit of time is μs) with units of mv μs.

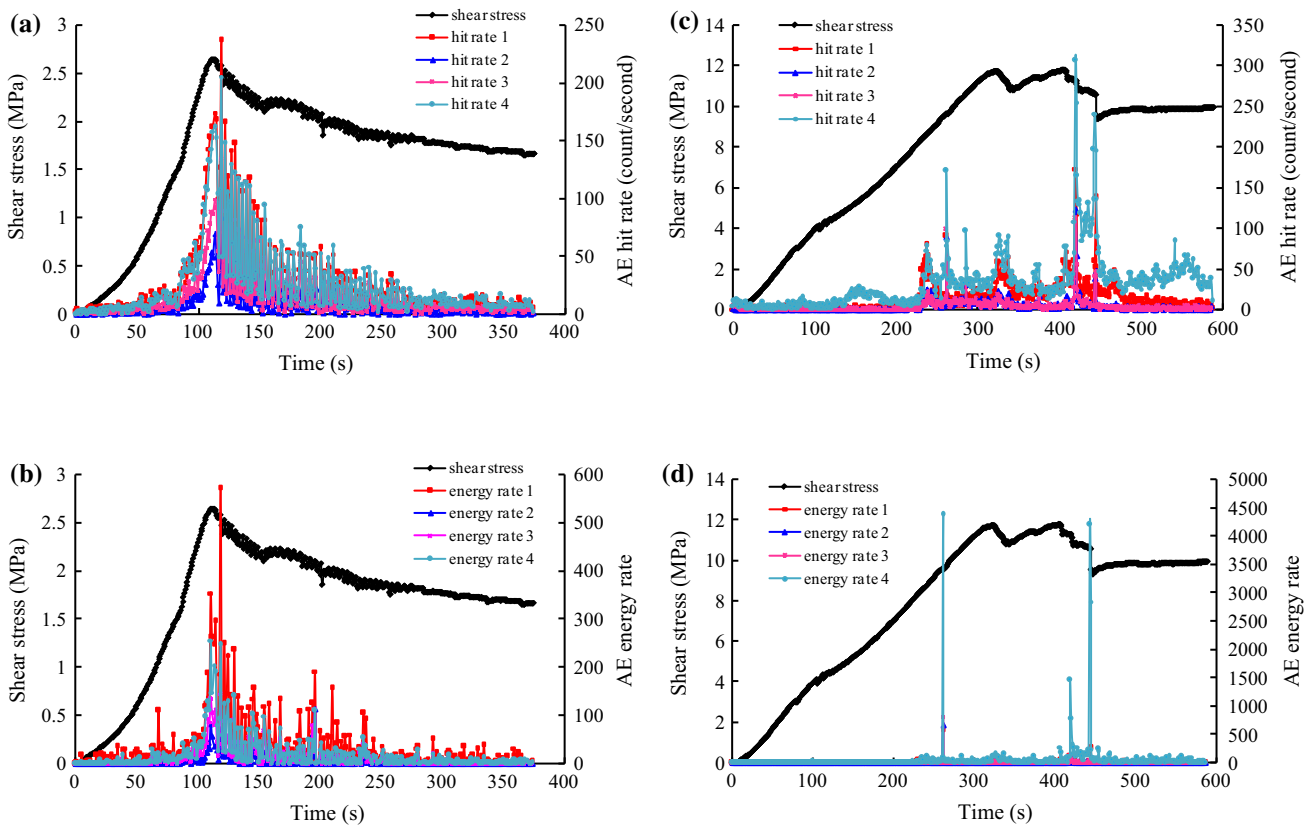

Fig. 5 Changes in the AE parameters with shear time for the cement mortar joints under 1 MPa (**a**, **b**) and 10 MPa (**c**, **d**) of normal stress: **a** and **c** show the hit rate, and **b** and **d** show the energy rate

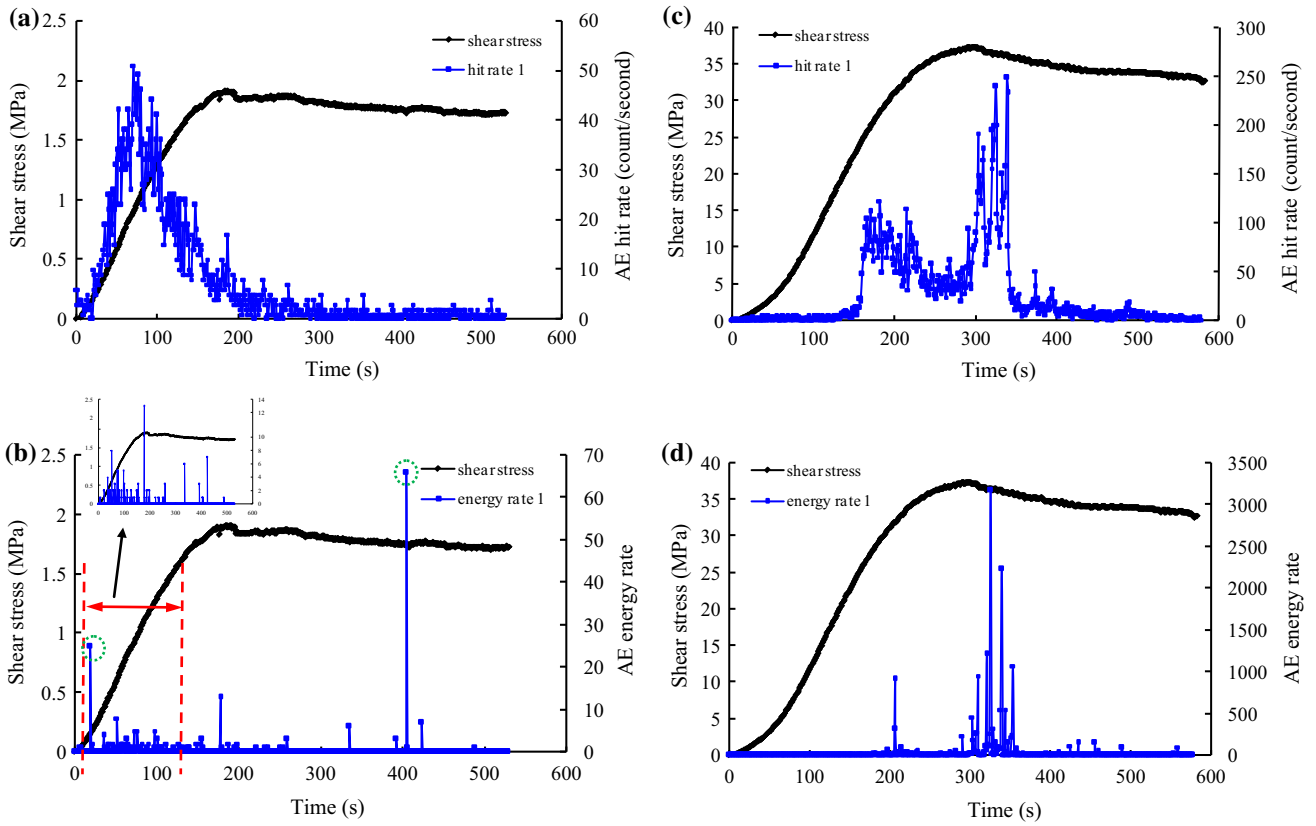

Fig. 6 Changes in the AE parameters with shear time for the marble joints under 1 MPa (**a**, **b**) and 40 MPa (**c**, **d**) of normal stress: **a** and **c** show the hit rate, and **b** and **d** show the energy rate

Figure 5a, b shows that the patterns of the AE hit rate and energy rate over time were almost identical, increasing with shear stress, peaking near the maximum shear stress, and gradually decreasing with time (the shear stress became strain weakening after peak stress). Subsequently, the values decreased to extremely low levels when the shear stress approached the ultimate shearing stage. The changes in the hit rate and energy rate that were monitored by the four sensors were consistent with one another, and the number of hits was not equivalent among the four sensors because of their different locations.

Figure 5c, d shows the AEs of cement mortar joints subjected to 10 MPa of normal stress and indicates that most of the hits and energy were radiated in the post-peak region. Moreover, as the shear stress curve fluctuated around the peak stress region, the patterns of the hits and energy rate became more complex than those observed under a normal stress of 1 MPa. Due to the local fractures and concentrated damage on the joint surface under high normal stress, the AEs peaked at the point of small stress drops.

Figure 6 demonstrates the AE hit and energy rates for marble joints when the normal stresses were 1 and 40 MPa. As shown in Fig. 6a, the hit rate increased with shear stress in the beginning when the normal stress was 1 MPa. However, unlike the patterns observed with cement mortar joints, the maximum hit rate was attained before the peak shear stress, and the AE hit rate became quiet during the ultimate sliding stage. In addition, the energy rate, as shown in Fig. 6b, was maintained at a low level throughout the entire shear process and was more active in the pre-peak period than in the post-peak stage. The change patterns of the two AEs indicated that inter mineral shear occurred before the peak shear stress. The two energy uprush points potentially resulted from local fracturing (such as the rotation and crushing of a fragment or mineral particle, or small local cracking), which emits few AE hits but with high energy. The small graph in Fig. 6b shows the results when the two points are neglected. Figure 6c, d shows the AEs for marble joints under 40 MPa of normal stress. The AEs became active before their peak stress, which indicated that some friction and slippage occurred between the adjacent minerals, and the hit rate and energy rate peaked near or slightly beyond the maximum shear stress due to the shear movement of the tightly interlocked joint surfaces.

Figure 7 shows the AEs for granite joints under 1 and 10 MPa of normal stress. The changes of AEs under a normal stress of 10 MP represent the stress curves with

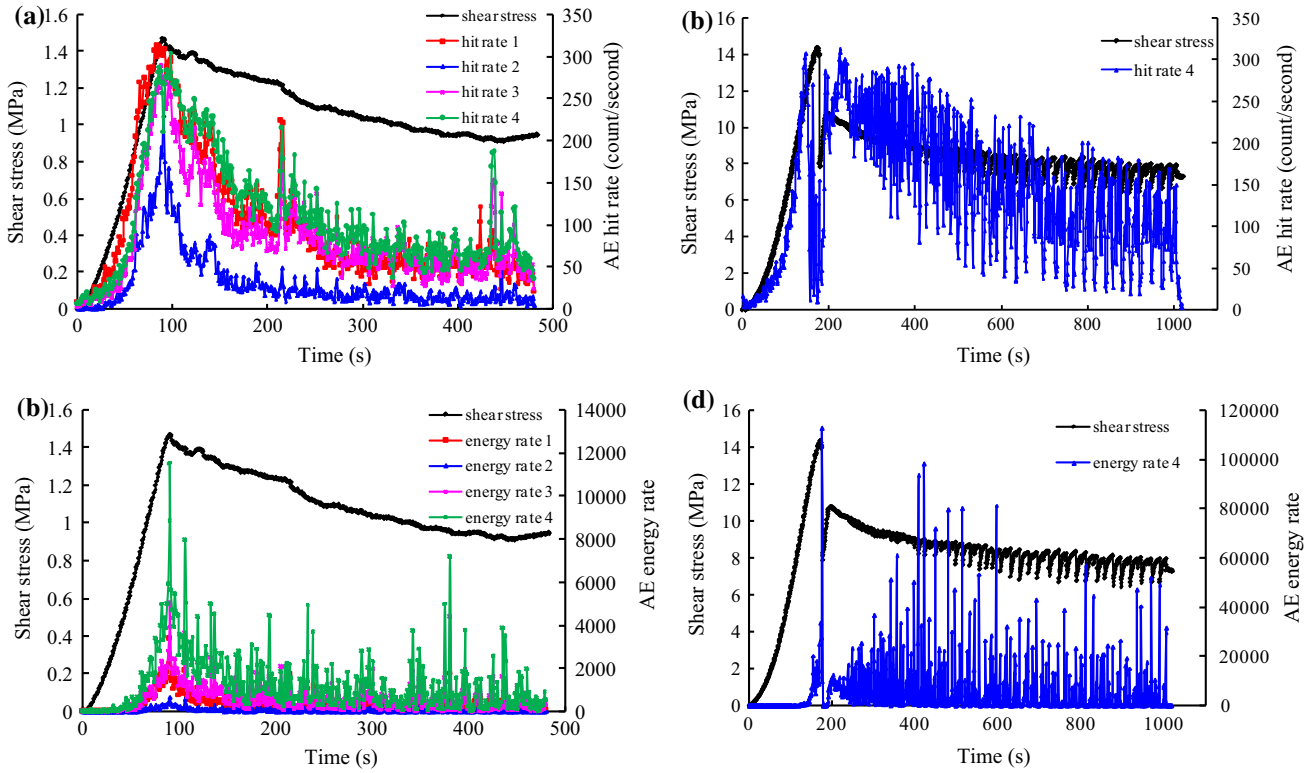

Fig. 7 Changes in the AE parameters with shear time for the granite joints under 1 MPa (**a**, **b**) and 10 MPa (**c**, **d**) of normal stress: **a** and **c** show the hit rate, and **b** and **d** show the energy rate

obvious periodic stress oscillations during the ultimate sliding period. The changes of the AE hit rate and energy rate under 1 MPa of normal stress are shown in Fig. 7a, b and were almost identical to the changes of the cement mortar joints at low normal stress, which are shown in Fig. 5a, b. The AEs increased with increasing shear stress and peaked almost simultaneously before decreasing gradually with time. Nevertheless, the AEs were much more active for the granite joints, and the number of hits and energy rate was higher than those of the cement mortar joints. Moreover, the AEs (particularly the energy rate) did not decrease continuously but surged at some point during the ultimate shear stage because of the crushing and rolling of the hard, stiff and brittle mineral compositions such as quartz and feldspar during frictional processes. Figure 7c, d shows the AEs for a normal stress of 10 MPa and demonstrate that a large amount of energy was released at the first violent post-peak stress drop, during which a very loud sound was recorded. The AEs during the post-peak sliding stage, particularly during stress oscillation, were also intense. At some points, the energy rate was even higher than the peak value under lower normal stresses and greater than that of most of the marble and cement mortar joints. The energy rate sharply increased at the moments of stress drops during the stress oscillation period and was accompanied by repeated loud noises.

4 Conclusions

Shear tests were conducted on tension marble, granite and cement mortar joints under various normal stresses (from 0.5 to 45 MPa) to investigate the shear behaviour and AE characteristics of different joints, and the following primary conclusions were drawn from these investigations:

1. The fewest AE events and the faintest dilation occurred for marble joints under low normal stress because the number of small-scale asperity on the surfaces was lacking, and the apparent cohesion was greater at higher normal stress levels due to the over-closure effect. The shear stress curves of the cement mortar joints fluctuated with increasing normal stress, and the curved ultimate strength envelope indicated that the mortar was collapsing under elevated normal stress because of its high porosity and loose structure.
2. The patterns of shear stress and AEs were similar between the cement mortar and granite joints under low normal stress, but the AEs of the granite joints were more active due to the crushing and rolling of the hard, stiff and brittle mineral compositions.
3. Violent post-peak stress drops occurred at normal stresses greater than 5 MPa, and periodic shear stress oscillations were observed at normal stresses greater

than 10 MPa for the granite joints. The energy rate sharply increased at the moments of stress drops, which was accompanied by repeated loud noises.

4. Dilation was the most prominent for the cement mortar joints under low normal stress. Apparent cohesion loss during failure was the greatest for the granite joints, which was consistent with the most violent brittle failure phenomena, and the AEs were the most active because of the brittle and hard mineral compositions.

Acknowledgments Financial support from the National Program on Key Basic Research Project of China under Grant No. 2014CB046902 and the National Natural Science Foundation of China under Grant Nos. 51279201, 41172288, 41472270 and 41372298 are gratefully acknowledged. The work in this paper was also supported by Open Research Fund of State Key Laboratory of Geomechanics and Geotechnical Engineering, Institute of Rock and Soil Mechanics, Chinese Academy of Sciences, Grant No. Z015007.

References

Barton N (1973) Review of a new shear strength criterion for rock joints. Eng Geol 7:287–332

Barton N, Choubey V (1977) The shear strength of rock joints in theory and practice. Rock Mech 10:1–54

Bewick RP (2013) Shear rupture of massive brittle rock under constant normal stress and stiffness boundary conditions. PhD thesis, University of Toronto, Toronto

Grasselli G (2006) Shear strength of rock joints based on quantified surface description. Rock Mech Rock Eng 39(4):295–314

Hong C, Seokwon J (2004) Influence of shear load on the characteristics of acoustic emission of rock-concrete interface. Key Eng Mater 270–273:1598–1603

Ladanyi B, Archambault G (1969) Simulation of the shear behavior of a jointed rock mass. In: Proceedings of the 11th US symposium on rock mechanics (USRMS), Berkeley, California, June 1969, pp 105–125

Meng FZ, Zhou H, Wang ZQ et al (2016) Experimental study on the prediction of rockburst hazards induced by dynamic structural plane shearing in deeply buried hard rock tunnels. Int J Rock Mech Min Sci 86:210–223

Moradian ZA, Ballivy G, Rivard P, Gravel C, Rousseau B (2010) Evaluating damage during shear tests of rock joints using acoustic emission. Int J Rock Mech Min Sci 47(4):590–598

Moradian ZA, Ballivy G, Rivard P (2012) Correlating acoustic emission sources with damaged zones during direct shear test of rock joints. Can Geotech J 49(6):710–718

Patton FD (1966) Multiple modes of shear failure in rock. In: Proceedings of the 1st congress of the international society of rock mechanics, Lisbon, Portugal, September/October 1966, vol 1, pp 509–513

Scholz CH (2002) The mechanics of earthquakes and faulting. Cambridge University Press, Cambridge

Xia CC, Tang ZC, Xiao WM, Song YL (2014) New peak shear strength criterion of rock joints based on quantified surface description. Rock Mech Rock Eng 47:387–400

Zhao J (1997) Joint surface matching and shear strength part B: JRC-JMC shear strength criterion. Int J Rock Mech Min Sci 34:179–185

Zhou H, Meng FZ, Zhang CQ et al (2014) Investigation of the acoustic emission characteristics of artificial saw-tooth joints under shearing condition. Acta Geotechnica. doi:10.1007/s11440-014-0359-3